AIP | Applied Physics Letters

Graphene as anode electrode for colloidal quantum dots based light emitting diodes

Alexander V. Klekachev, Sergey N. Kuznetsov, Inge Asselberghs, Mirco Cantoro, Jeong Hun Mun, Byung Jin Cho, André L. Stesmans, Marc M. Heyns, and Stefan De Gendt

Citation: Applied Physics Letters **103**, 043124 (2013); doi: 10.1063/1.4816745
View online: http://dx.doi.org/10.1063/1.4816745
View Table of Contents: http://scitation.aip.org/content/aip/journal/apl/103/4?ver=pdfcov
Published by the AIP Publishing

Graphene as anode electrode for colloidal quantum dots based light emitting diodes

Alexander V. Klekachev,[1,2,a)] Sergey N. Kuznetsov,[3] Inge Asselberghs,[1,4] Mirco Cantoro,[1,2] Jeong Hun Mun,[5] Byung Jin Cho,[5] André L. Stesmans,[2] Marc M. Heyns,[1,6] and Stefan De Gendt[1,4]

[1]*IMEC, Kapeldreef 75, B-3001 Leuven, Belgium*
[2]*Department of Physics and Astronomy, University of Leuven, Celestijnenlaan 200D, B-3001 Leuven, Belgium*
[3]*Department of Solid State Physics, Petrozavodsk State University, Lenin av. 33, 185910 Petrozavodsk, Russian Federation*
[4]*Department of Chemistry, University of Leuven, Celestijnenlaan 200F, B-3001 Leuven, Belgium*
[5]*Department of Electrical Engineering, KAIST, Daehak-Ro 291, DaeJeon 305-701, South Korea*
[6]*Department of Metallurgy and Materials Engineering, University of Leuven, Kasteelpark Arenberg 44, B-3001 Leuven, Belgium*

(Received 14 August 2012; accepted 9 July 2013; published online 26 July 2013)

Graphene films demonstrating low sheet resistance and high transparency in the visible light range are promising to be used as electrodes for light-emitting applications. In this work, we report the implementation of single layer graphene as hole injecting electrode for CdSe/ZnS quantum dot-light emitting diodes (QD-LED). We compare graphene vs. indium-tin-oxide (ITO)-based anode junctions by electroluminescence intensity performance of QD-LEDs. Our results demonstrate better hole injection efficiency for the graphene-based electrode at technologically relevant current densities $J < 0.4\ A/cm^2$, therefore, recommending single layer graphene as a valuable alternative to replace ITO in QD-LED technology. © *2013 AIP Publishing LLC*. [http://dx.doi.org/10.1063/1.4816745]

Graphene possesses unique physical properties, due to its specific energy bands configuration.[1] A single layer graphene absorbs ~2.3% in the visible light range, and has relatively low sheet resistance values combined with a strong, elastic crystalline lattice.[2] Taking into account the recent progress in large-scale graphene synthesis,[3,4] graphene is considered as a replacement for indium-tin-oxide (ITO) in multiple transparent electrode applications.[2] Nowadays, light emitting and light harvesting technologies widely employ ITO as a transparent electrode for carrier injection or extraction.[5] ITO possesses sheet resistance values, Rs, as low as 10 Ω/□ at a moderate light transmittance of 80%.[5] Besides the continuously increasing costs, ITO possesses several technological drawbacks, including high surface roughness due to its polycrystalline nature, work function instability under different processing conditions, and brittleness when applied for flexible devices.[5] Therefore, graphene is proposed as an alternative to replace ITO (Ref. 2) and it has already been efficiently applied in organic solar cells[6] and organic light-emitting diodes (OLEDs).[7]

Significant progress has been achieved over the past decade in the II–VI colloidal semiconducting quantum dots LED technology[8] utilizing CdSe/ZnS quantum dots (QDs) (and their derivatives such as ZnCdS/ZnS, CdZnSe) as active medium by optimizing the active layer formation, carrier injection, and buffer layers.[9,10] Discrete LEDs[11,12] and full-color displays[13] showing luminance values of up to several hundred thousands cd/m^2 and external quantum efficiencies of up to 7% were demonstrated.[11] All the studies referenced above utilize conventional ITO layers either as anode or cathode electrode. In this work, we employ graphene as a transparent electrode in QD-LEDs. We address the problem of electrode optimization by introducing single layer graphene as anode for simplified QD-LED structures. By comparing graphene- and ITO-based QD-LEDs, we demonstrate that single layer graphene can be used as an efficient anode junction electrode. Considering the chemical nature difference with ITO, the intrinsic flatness and the work function tunability by doping[14,15] of graphene make that the latter has every chance for being implemented as electrode material for QD-LEDs and related devices.

The graphene films employed in this work are synthesized by Cu-catalyzed chemical vapor deposition (CVD) resulting in a single-layer-thick graphene film over the whole area of a $Cu/SiO_2/Si$ wafer stack.[3,4] The obtained graphene is transferred to glass substrates by means of a poly(methyl methacrylate) (PMMA)-assisted transfer technique.[16–18] A uniform graphene film of $8 \times 8\ mm^2$ in size on glass is contacted in the Van der Pauw configuration by a Cr/Au layer (1 nm/80 nm) through shadow mask evaporation. All samples are characterized by Raman spectroscopy,[19] Hall effect, and optical transmittance measurements.[20] Sheet resistance measurements reveal values in the range of Rs = 900–1300 Ω/□ and a Hall mobility of $\mu_p = 800–1100\ cm^2/V\,s$. As evidenced by Hall effect measurements, the graphene samples exhibit weak p-doping, not exceeding the level of $p \sim 2 \times 10^{12}\ cm^{-2}$, which can be attributed to the presence of residuals on the graphene surface, e.g., transfer polymer particles. The variations in Rs from sample to sample are due to fluctuations in residual p-doping, and the number of micro-mechanical defects induced by graphene film manipulation during the transfer process. For ITO-based QD-LEDs, the same glass substrates were used, now covered with a 250-nm thick sputtered ITO layer (Rs ~ 20 Ω/□; optical transmittance T = 75% at λ = 550 nm).[20] The surface roughness of both electrode types has been monitored by atomic force

a)E-mail: alexander.klekachev@imec.be

microscopy (AFM)[20] giving RMS surface roughness values of 1.58 nm and 0.51 nm for ITO and graphene, respectively. Considering the values mentioned above, the prepared graphene samples are of a decent quality as compared to the literature data.[21] Core-shell CdSe/ZnS quantum dots (Evident Technologies, USA) with trioctylphosphine oxide (TOPO) ligands, exhibiting a photoluminescence (PL) peak at $\lambda \sim 596$ nm and a photoluminescence quantum yield of 70% are applied as active medium for QD-LEDs.

The QD-LED samples represent a simplified structure of similar devices as reported by Hikmet *et al.*[22] Depending on the anode junction and the active layer fabrication approach invoked, we distinguish three types of QD-LED devices schematically shown in Fig. 1(a). Each of them consists of an anode electrode (graphene or ITO), a hole-injection layer (HIL), and a QDs layer directly contacted with the cathode metal electrode (Fig. 1(a)). The anode junction in all cases is formed by alignment of the respective electrode with the poly(3,4-ethylenedioxythiophene) poly(styrenesulfonate) (PEDOT:PSS), a commonly used organic HIL.[22–24] While ITO shows rather good wetting by PEDOT:PSS, the graphene surface exhibits high water contact angles due to its hydrophobic non-polar nature. Despite some reports on difficulties in obtaining uniform PEDOT coverage of graphene,[25,26] it has been effectively implemented for the fabrication of large area OLEDs.[7] By the same procedure, we were able to produce homogenous PEDOT films on graphene without the presence of any dots or patchy areas. We obtain an identical yield of operational devices for both ITO- and graphene-based QD-LEDs. It is also important to take into account the two-fold role of PEDOT observed for the case of graphene-based QD-LEDs. The PEDOT layer not only facilitates hole injection into QDs but also acts as a strong p-dopant of graphene. Examining PEDOT-treated graphene layers by Hall measurements reveals a nearly four times increased hole concentration (reaching $p \sim 2 \times 10^{13}\,cm^{-2}$) accompanied by a three times decrease in sheet resistance Rs as compared to the pristine graphene.[20] The doping of graphene results in a shift of its Fermi level E_F that is calculated[1] via $E_F = \sqrt{p\pi}\hbar v_F$, where $p \sim 2 \times 10^{13}\,cm^{-2}$ is the excess of charge in graphene, $v_F = 10^6$ m/s is Fermi velocity, and $\hbar$ is the reduced Planck constant. The work function of 4.4–4.5 eV (Ref. 27) reported for pristine graphene is shifted by the p-doping to the 4.8–4.9 eV range (Fig. 1(b)).

After the formation of the anode junction, a layer of QDs is spin coated from solution on top of the PEDOT layer. For the graphene QD-LED device type 1, we followed the literature approach of embedding QDs in conventional polyimide polymer grafted with additives to enhance hole transport.[24,28] In this case, the conductive polymer matrix provides transport paths for holes and to some extent for electrons to the QDs. Additionally, the polymer is encapsulating the QDs to protect them from the ambient, especially oxygen and water vapor which adversely affect the QDs performance during device operation. However, the encapsulating polymer often screens the real characteristics and working of QDs in the structure.[24,28] Therefore, to compare ITO and graphene, we focus on the samples prepared only with bare QDs as active layer, but having graphene (device type 2) and ITO-based anode junctions (device type 3), respectively. In all cases, the thickness of the active layer is around 30–40 nm (as determined by ellipsometry) which corresponds to the QDs multilayer.

The device fabrication is completed by thermal evaporation of a 100 nm thick aluminum layer through a shadow mask resulting in an array of cathode junctions of 0.7×0.7 mm^2. A schematic energy level diagram for a type 2 graphene-based QD-LED device is shown in Fig. 1(b). Positively biased graphene combined with PEDOT HIL injects holes, whereas that Al cathode injects electrons into the QDs.

PL and electroluminescence (EL) spectroscopy methods are used to characterize the structures. In both cases, the emitted light is coupled to a grating monochromator with a CCD-camera. All optical measurements are performed at spectral resolution of 1 nm and a CCD accumulation time of 1 s. A He-Cd laser (325 nm line) is used for the photoluminescence measurements. Electroluminescence excitation is carried out by using a constant current source with variable output, in this way ensuring a galvanostatic operation regime for the samples under study.

We first focus on the characterization of device type 1. Fig. 2(a) shows current density-voltage (J–V) characteristic in the forward regime (positive bias at the graphene electrode). This curve shows no visible rectification in the EL-active region of J and is demonstrating symmetric ($J < 0$ part is not shown) nearly ohmic behavior ($J \propto V^{0.96}$) typical for the bulk-limited conduction[22] with an extrapolated bias threshold of $V_{th} = 4.6$ V. Similar to the report by Hikmet *et al.*,[22] the electroluminescence can be induced not only by applying the forward current but is also found to appear in

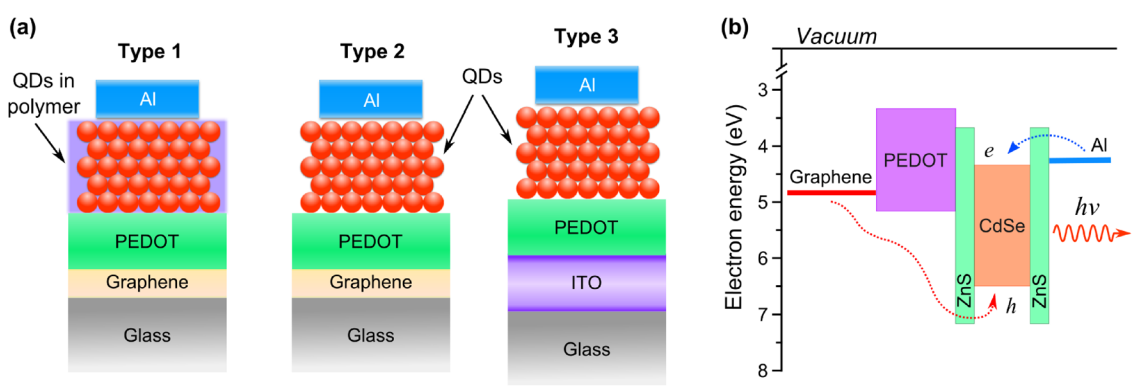

FIG. 1. (a) Schematic representation of the types of QD-LED structures under study; (b) the energy band diagram of the QD-LED device type 2.

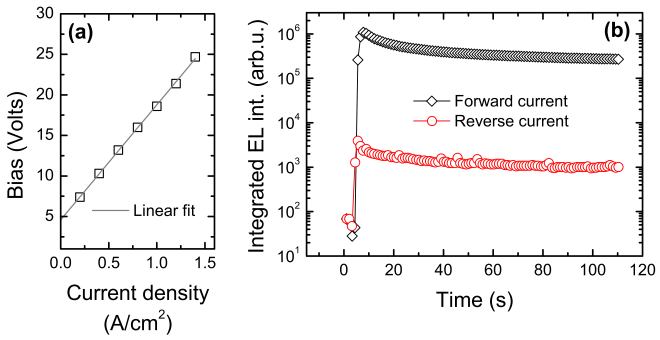

FIG. 2. Shown for the type-1 devices is: (a) J–V characteristic (open squares) and its linear fit (gray line). (b) EL intensity kinetics under forward (black squares) and reverse (red circles) current density of J = 0.2 A/cm^2 for both cases.

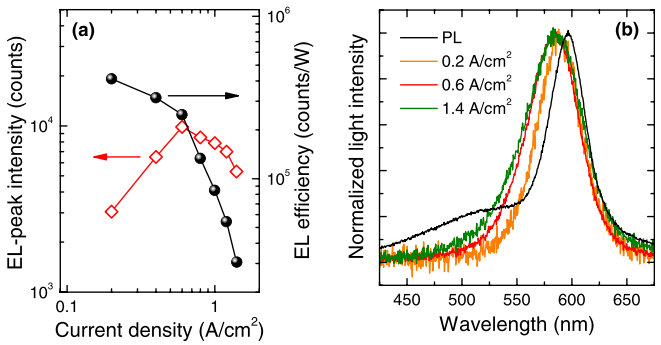

FIG. 3. Shown for the type-1 devices is: (a) EL-peak intensity (red line) and EL power efficiency (black line) vs current density in a log-log plot. (b) Normalized EL spectra shown for selected J values together with a photoluminescence spectrum observed on the as-fabricated sample.

the reversed current regime when the graphene electrode is under negative bias (Fig. 2(b)). As seen from Fig. 2(b), the forward regime yields significantly higher EL efficiency than the reversed one. This observation is in accordance with the energy level diagram shown in Fig. 1(b): The positively biased Al cathode makes hole injection difficult. Therefore, the drastically suppressed EL in the reverse regime is an indication of the significant imbalance between hole and electron currents as compared to the case of forward current operation. However, even in the forward regime, device operation is limited to the range of J where the EL intensity is proportional to the applied current density.

Fig. 3(a) shows the QDs electroluminescence peak intensity as a function of J. The EL intensity increases proportional to J at moderate current densities followed by decreased EL signal at J > 0.6 A/cm^2. Further increase of J results in the appearance of significant hole and electron currents imbalance. As also seen from Fig. 3(a), within our experimental conditions, we are able to scan only the roll-off part of the device electroluminescence power efficiency curve. The maximum of the EL power efficiency for QD-LEDs is often observed in the range of J = 10–300 mA/cm^2.[9,11,29,30] Fig. 3(a) indicates that the maximum of EL power efficiency is located at J ≤ 0.2 A/cm^2. Therefore, taking into consideration the EL peak intensity curve, we can define J ≲ 0.6 A/cm^2 as the upper operating current density limit for the QD-LED structures employed in this work. Fig. 3(b) shows a set of EL spectra observed at different J values, where a photoluminescence spectrum of the as-fabricated structure is also plotted for comparison. The PL spectrum reveals two components: a QD emission peak centered at $\lambda \sim 596$ nm and a polymer peak centered at $\lambda \sim 558$ nm. As seen from Fig. 3(b), the short-wavelength side of the EL peaks is drastically blue-shifted while the long-wavelength exhibits only a minor shift relative to PL peak. The former shift is independent of the anode type and the presence of polymer in the active layer. This observation is further discussed in Sec. 3 of supplementary information.[20]

We now turn to the characterization of the devices type 2 (graphene anode) and type 3 (ITO anode) having a bare QDs coating as an active layer. Fig. 4 compares the performance of the QD-LEDs type 2 and 3, showing the dependence of integrated EL intensity vs. current density. As seen from Fig. 4(a), device type 2 shows a stronger EL signal only for J below about 0.35 A/cm^2, while the type 3 device clearly outperforms for J > 0.4 A/cm^2. Figure 4(b) presents a more detailed scan over the current density region J = 0–0.35 A/cm^2. A nearly five times stronger EL signal observed for graphene-based QD-LED at J = 0.2 A/cm^2. As mentioned before, the typical active current density region for QD-LEDs is lying in the range of J = 10–300 mA/cm^2. This observation can be explained in terms of the work function difference between the two anode materials. The work function of ITO is reported to be in the range of 4.5–4.7 eV,[31,32] while the Fermi level for the case of p-doped graphene is $E_F \sim 4.8$–4.9 eV. Since the latter is closer to the highest occupied molecular orbital (HOMO) of PEDOT (5.1–5.2 eV), the process of hole

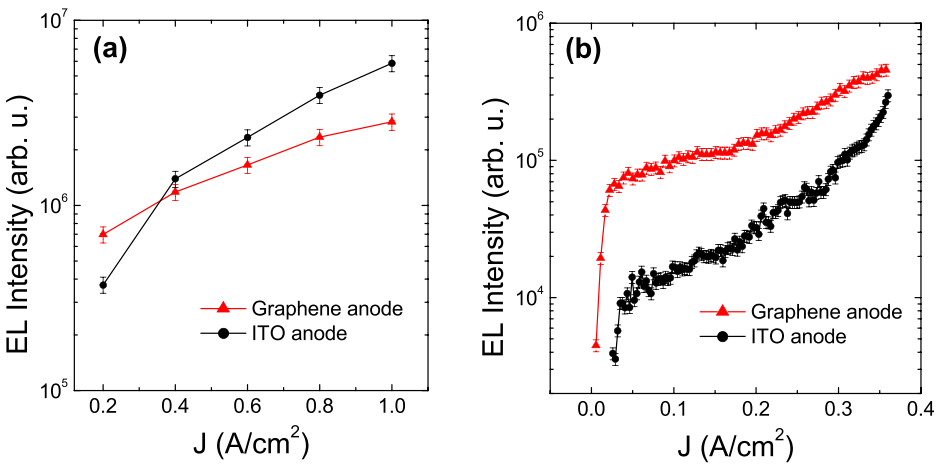

FIG. 4. Integrated EL intensity of QD-LED with graphene (type 2; triangles) and ITO based (type 3; circles) anode junctions as a function of current density for the (a) complete current density range, and (b) a detailed scan for current densities J < 0.35 A/cm^2.

injection from graphene is more favorable than that in the case of ITO. We assume this difference is responsible for stronger EL intensity of graphene-based QD-LED at $J < 0.4\ A/cm^2$.

Additionally, the following interpretation for the stronger EL intensity from device type 3 compared to device type 2 in the high current density region can be forwarded. Indium tin oxide films, typically, prepared by magnetron sputtering have a polycrystalline nature known to exhibit a rough spike-like surface[20,33] (see AFM profiles of ITO surface in the Supplementary Information file). We then hypothesize that the spike-like grains of ITO can result in the formation of domains of high local electric field giving rise to a higher injection capability of ITO at higher J. However, these features will also promote current crowding through the device and, hence, may result in an increased degradation rate of the device active layer. The above mentioned process would not take place in the case of graphene-based (type 2) devices because of the intrinsic flatness of graphene and thus represents another beneficial property of graphene as electrode material for QD-LEDs.

Our results can be compared to the report by Han *et al.*, implementing doped few-layer graphene films in OLED structures.[7] It is shown there that the 4-layer graphene stacks employing a sophisticated doping technique can outperform ITO-based OLED, while the performance of the 2-layer graphene based OLED is appreciably low. In contrast, our findings evidence that a single layer of graphene shows better performance than ITO in the QD-LED applications at practically relevant current densities.

In conclusion, we report on the operation of a graphene-anode based colloidal quantum dot light emitting diode structure. The results acquired on our devices demonstrate that single layer graphene films are very promising for ITO replacement in QD-LEDs in the range of current densities that is typically used in QD-LED operation. Taking into account the tunability of the work function of graphene, it can be used in both anode and cathode junctions. Nevertheless, improvement of the wafer-scale graphene synthesis and transfer techniques is still necessary. Together with the search for increasing the quantum efficiency of QD-LEDs, it should be the subject of the future work.

S.N.K. gratefully acknowledges financial support by the Program for Strategic Development of Petrozavodsk State University. B.J.C. acknowledges financial support from Korean NRF research Grant No. 2010-0029132.

[1]A. H. Castro Neto, F. Guinea, N. M. R. Peres, K. S. Novoselov, and A. K. Geim, Rev. Mod. Phys. **81**, 109 (2009).
[2]F. Bonaccorso, Z. Sun, T. Hasan, and A. C. Ferrari, Nature Photon. **4**, 611 (2010).
[3]J. K. Park, S. M. Song, J. H. Mun, and B. J. Cho, Nano Lett. **11**, 5383 (2011).
[4]T. Yoon, W. C. Shin, T.-S. Y. Kim, J. H. Mun, and B. J. Cho, Nano Lett. **12**, 1448 (2012).
[5]D. S. Ginley, H. Hosono, and D. C. Paine, *Handbook of Transparent Conductors*, 1st ed. (Springer, New York, 2010), p. 534.
[6]X. Miao, S. Tongay, M. K. Petterson, K. Berke, A. G. Rinzler, B. R. Appleton, and A. F. Hebard, Nano Lett. **12**, 2745 (2012).
[7]T.-H. Han, Y. Lee, M.-R. Choi, S.-H. Woo, S.-H. Bae, B. H. Hong, J.-H. Ahn, and T.-W. Lee, Nature Photon. **6**, 105 (2012).
[8]Y. Shirasaki, G. J. Supran, M. G. Bawendi, and V. Bulović, Nature Photon. **7**, 13 (2012).
[9]J. W. Stouwdam and R. A. J. Janssen, J. Mater. Chem. **18**, 1889 (2008).
[10]V. Wood, M. J. Panzer, J. E. Halpert, J. M. Caruge, M. G. Bawendi, and V. Bulovic, ACS Nano **3**, 3581 (2009).
[11]J. Kwak, W. K. Bae, D. Lee, I. Park, J. Lim, M. Park, H. Cho, H. Woo, D. Y. Yoon, K. Char, S. Lee, and C. Lee, Nano Lett. **12**, 2362 (2012).
[12]P. O. Anikeeva, J. E. Halpert, M. G. Bawendi, and V. Bulovic, Nano Lett. **9**, 2532 (2009).
[13]T.-H. Kim, K.-S. Cho, E. K. Lee, S. J. Lee, J. Chae, J. W. Kim, D. H. Kim, J.-Y. Kwon, G. Amaratunga, S. Y. Lee, B. L. Choi, Y. Kuk, J. M. Kim, and K. Kim, Nature Photon. **5**, 176 (2011).
[14]W. Chen, S. Chen, D. C. Qi, X. Y. Gao, and A. T. S. Wee, J. Am. Chem. Soc. **129**, 10418 (2007).
[15]L. Bing, A. V. Klekachev, M. Cantoro, C. Huyghebaert, A. Stesmans, I. Asselberghs, S. De Gendt, and S. De Feyter, "Toward tunable doping in graphene FETs by molecular self-assembled monolayers," Nanoscale (published online).
[16]S. Bae, H. Kim, Y. Lee, X. Xu, J.-S. Park, Y. Zheng, J. Balakrishnan, T. Lei, H. R. Kim, Y. Il Song, Y.-J. Kim, K. S. Kim, B. Ozyilmaz, J.-H. Ahn, B. H. Hong, and S. Iijima, Nat. Nanotechnol. **5**, 574 (2010).
[17]A. Srivastava, C. Galande, L. Ci, L. Song, C. Rai, D. Jariwala, K. F. Kelly, and P. M. Ajayan, Chem. Mater. **22**, 3457 (2010).
[18]X. Li, Y. Zhu, W. Cai, M. Borysiak, B. Han, D. Chen, R. D. Piner, L. Colombo, and R. S. Ruoff, Nano Lett. **9**, 4359 (2009).
[19]A. C. Ferrari and D. M. Basko, Nat. Nanotechnol. **8**, 235 (2013).
[20]See supplementary material at http://dx.doi.org/10.1063/1.4816745 for graphene synthesis and characterization details, PEDOT:PSS deposition on graphene and doping of graphene, and discussion over the EL-peak broadening.
[21]C. Mattevi, H. Kim, and M. Chhowalla, J. Mater. Chem. **21**, 3324 (2011).
[22]R. A. M. Hikmet, D. V. Talapin, and H. Weller, J. Appl. Phys. **93**, 3509 (2003).
[23]H. Mattoussi, L. H. Radzilowski, B. O. Dabbousi, E. L. Thomas, M. G. Bawendi, and M. F. Rubner, J. Appl. Phys. **83**, 7965 (1998).
[24]J. Zhao, J. Zhang, C. Jiang, J. Bohnenberger, T. Basché, and A. Mews, J. Appl. Phys. **96**, 3206 (2004).
[25]P. Hyesung, A. R. Jill, K. Ki Kang, B. Vladimir, and K. Jing, Nanotechnology **21**, 505204 (2010).
[26]H. Park, P. R. Brown, V. Buloyic, and J. Kong, Nano Lett. **12**, 133 (2012).
[27]R. Czerw, B. Foley, D. Tekleab, A. Rubio, P. M. Ajayan, and D. L. Carroll, Phys. Rev. B **66**, 033408 (2002).
[28]M. Y. Gao, B. Richter, S. Kirstein, and H. Mohwald, J. Phys. Chem. B **102**, 4096 (1998).
[29]S. Coe, W.-K. Woo, M. Bawendi, and V. Bulovic, Nature **420**, 800 (2002).
[30]Q. Sun, Y. A. Wang, L. S. Li, D. Wang, T. Zhu, J. Xu, C. Yang, and Y. Li, Nature Photon. **1**, 717 (2007).
[31]Y. Park, V. Choong, Y. Gao, B. R. Hsieh, and C. W. Tang, Appl. Phys. Lett. **68**, 2699 (1996).
[32]J. Cui, A. Wang, N. L. Edleman, J. Ni, P. Lee, N. R. Armstrong, and T. J. Marks, Adv. Mater. **13**, 1476 (2001).
[33]U. Betz, M. Kharrazi Olsson, J. Marthy, M. F. Escolá, and F. Atamny, Surf. Coat. Technol. **200**, 5751 (2006).